Analysis of the Adjacent Re-Entry Folds in the Form I of Syndiotactic Polypropylene

Roberto Napolitano and Beniamino Pirozzi*

Dipartimento di Chimica, Università di Napoli Federico II, via Mezzocannone 4, 80134 Napoli, Italy

Received December 29, 1997; Revised Manuscript Received February 23, 1998

ABSTRACT: Models of possible adjacent re-entry chain folds for the most stable form (form I) of syndiotactic polypropylene in the body-centered orthorhombic unit cell have been studied by molecular mechanics. Folds along (100), (010), and (110) planes connecting chains having both the same or the opposite chirality have been investigated. Various models of folds with different number of bonds have been built up and optimized by conformational energy calculations. Tight folds are the lowest in energy. Low-energy folds are possible along the three fold planes with some restrictions on the chirality of the chains. The energy values obtained for the best folds are in good agreement with the work of the fold deducible from experimental determinations. The energy calculations also indicate that configurational defects can be well tolerated in the fold.

Introduction

The recent development of new soluble metallocene catalyst systems[1] has allowed the synthesis of polyolefines having a very high degree of syndiotacticity. As a consequence, a large number of papers concerning structural studies of syndiotactic polyolefines have been published in the past decade.[2−16]

As far as syndiotactic polypropylene (sPP) is concerned, the higher configurational regularity has resulted in more regular crystals and new crystalline forms.[3,5−6] The various crystalline forms of sPP are characterized both by different conformations and by different modes of packing of chains having the same conformation. The most stable form, defined as form I,[13] is composed of chains of both chiralities having a **s(2/1)2** symmetry. Lotz et al.[3] proposed for this form an orthorhombic unit cell with $a = 14.50$ Å, $b = 11.20$ Å and $c = 7.40$ Å in the space group *Ibca*, for which chains having opposite chirality alternately succeed along both the *a* and the *b* axis, as shown in Figure 1. Overall, this structure is in good agreement with the diffraction data. However, it does not explain some discrepancies in the X-ray spectra and the splitting of the resonance of the methyl carbons observed in the NMR spectra.[17] Subsequently, De Rosa et al.[13] proposed the space group $P2_1/a$ with unit cell constants almost unchanged and with the positions of the chain axes practically the same as in the space group *Ibca*, but with the chains rotated ≈5° around the *c* axis and shifted ≈0.07*c* along the chain axis. The experimental discrepancies can be also explained by postulating a regular alternation of chains of opposite chirality along the *b* axis with a statistical disposition of chains having the same or the opposite chirality along the *a* axis,[16] in such a way that chains having the same chirality and chains having the opposite chirality are related as in the *Bbab* and in the *Ibca* space groups, respectively. A very recent paper by Lovinger and Lotz,[18] based on the analysis of literature data, reaffirms the choice of *Ibca* as the prototypical cell to describe the basic structure of form I of sPP.

The study of the crystal structure of sPP can be extended by an analysis of the folds, to clarify the characteristic of the interface between the crystal and the amorphous regions. The nature of folding in polymer chains is still an open question[19,20] because neither the degree of adjacent re-entry folds for the different kinetics of crystallization nor the lengths of the folds are well defined. On the other hand, recent experimental techniques, such as atomic force microscopy and cross-polarization MAS NMR, are helpful in the suggestion of reasonable hypotheses for the conformation of polymer chains in folds. Chain folding can be also studied by molecular mechanics. This kind of analysis finds the possible fold planes, the fold conformations, and the corresponding energies. It was applied in the past to different polymers.[21−29]

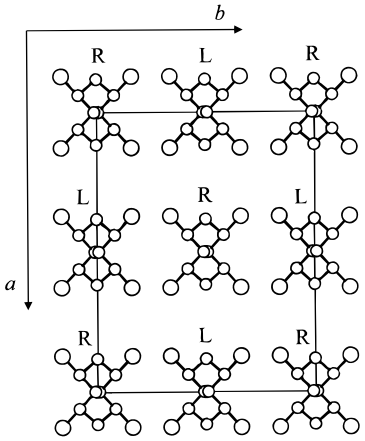

Figure 1. View along the *c* axis of the unit cell of sPP in the space group *Ibca*. R and L indicate right- and left-handed helixes, respectively.

In recent times, papers on the morphology of sPP have been published by several authors[30−37] some of which suggest the possible fold planes and give an evaluation of the work required to create a fold. Lovinger et al.[31,32] performed studies by electron diffraction and microscopy on decorated films and suggested that the folds are overwhelmingly disposed along the *b* axis, i.e., along (100) planes. This conclusion was supported by atomic force microscopy studies.[34] Subsequently, Bu et al.[37] investigated lamellar single crystals of sPP by transmission electron microscopy, atomic force microscopy,

S0024-9297(97)01872-X CCC: $15.00
Published on Web 05/12/1998

and electron diffraction and concluded that folds are also possible along (010) and (110) planes.

In this paper we report an analysis by molecular mechanics of the possible models of adjacent re-entry chain folding of form I of sPP, based on the proposed structures and fold planes. To this end, we have postulated models of folds which have been optimized by conformational energy calculations in order to find the best internal parameters and the lowest energies. The results also suggest the preferred fold planes and provide a theoretical value of the work of folding.

Analysis of Starting Models

The theoretical study of the chain folding requires both a geometry and an energy analysis. In fact a folded polymer chain has to fulfill two conditions: (i) the sequence of the internal parameters should not produce strong repulsive interactions; (ii) the atoms must assume the exact crystallographic position when the chain re-enters the crystal.

Due to the various structures proposed for sPP and to the various possible fold planes, several geometrical relations between adjacent chains should be considered. In fact, the distance between the chain axes depend on the fold plane, while the chiralities and the relative heights of adjacent chains depend on the particular crystal structure. The geometrical constraints limit the number of possible conformations of each fold, such that the choice of suitable starting models is critical. We have solved this problem by using three-dimensional molecular models reproducing in scale the polymer chains, built up around parallel rigid chain axes which were placed at the crystallographic distances and positions according to the unit cell proposed by Lotz et al.[3]

For each model we have chosen as fold surface a plane perpendicular to the chain axes, in such a way that the atomic groups below this plane were in crystallographic positions and groups above this plane belonged to the fold. We have observed that the number of bonds of the fold has to be not too large in order to achieve a low number of defects but sufficiently high to have enough degrees of freedom and, therefore, more ways of satisfying the geometrical constraints. Depending on the kind of fold, its length is the result of a compromise between these two opposite conditions.

Each model of fold is constituted by an initial stem having regular conformation, henceforth named the starting chain, by a central portion having nonregular conformation that represents the fold, and by a final stem having regular conformation, henceforth named the end chain. For all the models of fold, the starting chain has internal parameters corresponding to the minimum conformational energy of a R helix having **s-(2/1)2** symmetry, as reported in a previous paper.[16] This chain has been positioned at the origin of the unit cell for the structure represented in Figure 1 in such a way that the 2-fold axes of the helix are parallel to the *a* and *b* axes of the unit cell.

Figure 2 shows a schematic representation of a folded chain with the numbering of the internal parameters of the fold and the indication of the configurational signs of the bonds.[38]

We have examined the possible adjacent re-entry folds along the (100), (010), and (110) planes as sketched in Figure 3. For all the fold planes we have considered as end chain both a chain of opposite chirality (L) and a chain of the same chirality (R), related to the starting

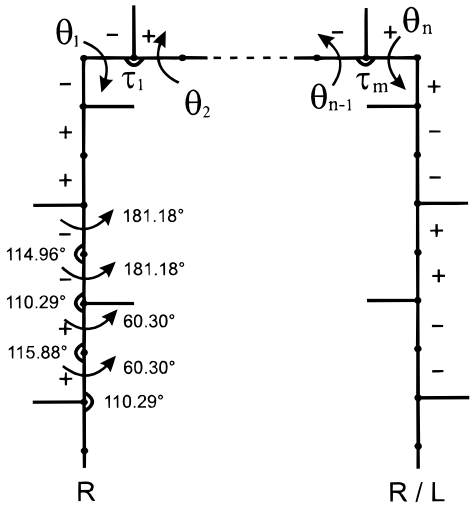

Figure 2. Schematic representation of a folded sPP chain. The vertical stems represent the starting (R) and the end (R or L) chain. The horizontal stem represents the fold with the indication of the variable torsion (θ_i) and bond (τ_i) angles in the backbone. The configurational signs of the bonds and the values of the internal parameters of the R regular chain are also reported.

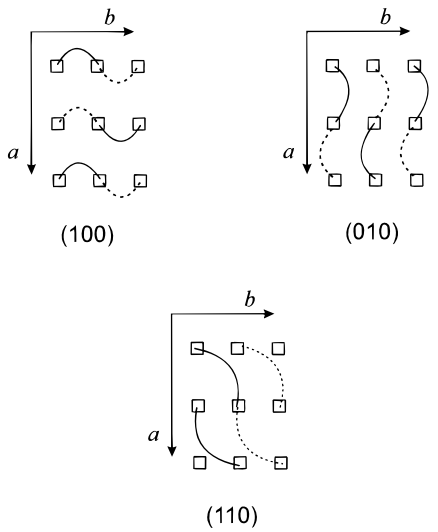

Figure 3. Sketches of the adjacent re-entry folds considered, with an indication of the corresponding fold planes.

chain by an inversion center or by a translation, respectively. For each fold plane and chirality the coordinates of the inversion center and the translation vector are those which determine the best mode of packing between regular chains in accordance with the previous packing energy calculations.[16] For the fold along (100) planes, the coordinates of the inversion center are $(0,{}^1/_4,{}^1/_4)$ and the translation is $b/2$.[39] The chain axes are therefore at the distance 5.60 Å. For the fold along (010) planes, the coordinates of the inversion center are $({}^1/_4,0,0)$ and the translation is ${}^1/_2(a+c)$. Therefore the chain axes are at the distance $a/2$, equal to 7.25 Å. For the fold along the (110) planes the coordinates of the inversion center are $({}^1/_4,{}^1/_4,0)$ and the translation is ${}^1/_2(a + b + c)$. The distance between the chain axes is therefore ${}^1/_2(a + b)$, equal to 9.36 Å.

For each fold we have built up models differing in the position of the fold surface, in the number of bonds and in the sequence of values of torsion angles. We have examined only the models for which the end chain is

close to the crystallographic position, and we have excluded the folds which had short distances between nonbonded atoms. These models were chosen as starting points for the energy minimizations. The values of the torsion angles of the selected models were visually estimated. The starting values of the bond angles were those of the regular chain in the crystal.

Method of Calculation

The models of fold devised as described in the previous section were optimized by varying all the torsion and bond angles both in the backbone and in the side groups. However, a local C_{2v} symmetry was maintained on methylene groups, and the methyl groups were considered as single units.

The optimizations of the models were performed by minimizing the energy of the polymer chain, calculated as $E = E_b + E_t + E_{nb} + E_p$. The term $E_b = {}^1/_2K_b(\tau - \tau_o)^2$ is due to the deformation of bond angles τ, the term $E_t = {}^1/_2K_t(1 + \cos 3\theta)$ is due to the intrinsic torsional potential for torsion angles θ, the term $E_{nb} = Ar^{-12} - Br^{-6}$ is due to the interactions between nonbonded atomic species at a distance r and with a separation of more than two bonds. The nonbonded term has been calculated by taking into account the interactions between the atoms inside the fold and the interactions between these atoms and those of the starting and of the end chain, calculated for distances less than twice the van der Waals distance for each pair of atomic species. The interactions between the atoms of the regular portions of the chain have been excluded. Besides the set of Flory parameters already used in ref 16, we have also utilized the softer set of parameters given by Scheraga[40,41] in order to evaluate the influence of the choice of the potential functions on the values of the internal coordinates and of the energy of the fold. The parameters of the potential functions are reported in Table 1. The term $E_p = K_p(\Delta x^2 + \Delta y^2 + \Delta z^2)$ is a penalty term which forces the end chain to assume the crystallographic position. K_p is an arbitrary constant and Δx, Δy, and Δz are the differences in the Cartesian frame between the actual and the crystallographic coordinates of a given atom of the re-entering chain. To make sure that all the atoms of the end chain assume the crystallographic positions, we have applied the penalty term to a triplet of nonaligned atoms which should be on lattice sites. We consider that the geometry constraints are satisfied when Δx, Δy, and Δz for the three chosen atoms are ≤ 0.15 Å. The conformational energy is then given by $E_{conf} = E - E_p$.

Due to the complexity of the system, the minimizations of the energy were performed in various consecutive steps. In fact, both geometry and energy conditions must be simultaneously satisfied and a large number of variables have to be optimized for all the folds. For instance, 31 parameters, 15 in the main chain and 16 determining the positions of the hydrogen atoms and of the methyl groups, were varied for the shortest fold (eight bonds) studied. Therefore, in the first step we used a low value of K_p and considered as variable parameters only the backbone torsion and bond angles. In the subsequent steps the other variable parameters were also taken into account, and higher values of K_p were used until the chosen geometry conditions were reached.

We have evaluated the energy required to fold a chain as $E_{fold} = E_{conf} - E_{rif}$ where E_{rif} is the minimum conformational energy of a regular chain with **s(2/1)2** symmetry having the same length as the fold. The value of E_{fold} can be compared with the work of folding obtained from experimental measurements.

Table 1. Parameters of the Potential Functions Used in the Energy Calculations[a]

Bending Terms

bond angle	K_b	τ_o
C−C−C	0.184	109.47
C−C−H	0.121	109.47
H−C−H	0.100	109.47

Torsional Terms

torsion angle	K_t
C−C−C−C	11.7

Nonbonded Terms (Flory)

interacting pair	$10^{-3}A$	B	d_w
C, C	1653	1519	3.6
C, H	236	531	3.1
C, CH_3	4018	2669	3.8
H, H	30.2	196	2.6
H, CH_3	613	950	3.3
CH_3, CH_3	9664	4719	4.0

Nonbonded Terms (Scheraga)

interacting pair	$10^{-3}A$	B	d_w
C, C	1197	1548	3.4
C, H	159	536	2.9
C, CH_3	1925	1698	3.6
H, H	18.7	195	2.4
H, CH_3	275	602	3.1
CH_3, CH_3	3059	1862	3.8

[a] The symbols are referred to the formulas reported in the text. The values of K_b, K_t, A, and B are expressed in such a way that the energy is in kJ·mol^{-1}, if angles and distances are expressed in deg and Å, respectively. d_w is the van der Waals distance.

Results

The conformational energies of all the starting models of fold were minimized. The values of the parameters of the backbone at the minimum energy point, obtained by using the nonbonded terms reported by Flory, are listed in Table 2. The (100) R, R and (110) R, L folds present larger deviations of the bond angles and a higher number of deviations of torsion angles from the values for a regular helix. For the other folds these deviations are present in a lesser extent and are reasonable for a fold that is not a regular chain. The minimum energy conformational parameters obtained using the Scheraga nonbonded terms are very similar to those reported in Table 2. The greatest deviations of torsion and bond angles are less than 15 and 3°, respectively. The values of the energy of the best folds obtained with the two sets of potential functions are reported in Table 3.

The results in Table 3 show that the energy values obtained using the Scheraga terms are lower than the corresponding values obtained using the Flory terms, since the Flory potential is stiffer. The energy difference obtained with the two functions for each fold is acceptable and the relative stability of the folds remains unchanged. The highest discrepancy in the energy values is for the (110) R, L fold. This fold and the (100) R, R fold are the highest in energy and have the highest deviations of the internal parameters with respect to a regular chain. Therefore, we think that the presence

Table 2. Values of the Torsion and Bond Angles (deg) in the Minimum Energy Points for the Indicated Fold Planes and Chiralities of the Chains

fold plane	chiralities	θ_1	θ_2	θ_3	θ_4	θ_5	θ_6	θ_7	θ_8	θ_9	θ_{10}	θ_{11}	θ_{12}
100	R, L	−134	−64	153	−74	−141	72	70	−89	−113	162		
100	R, R	−81	−148	82	60	−118	172	157	152	−156	73	84	−129
010	R, L	165	−153	37	51	−167	163	164	165	−99	164	164	173
010	R, R	179	176	163	−125	57	104	149	179				
110	R, L	132	106	−144	−155	177	167	178	52	−83	163	−155	−60
110	R, R	151	61	154	−178	−171	70	111	−76	−79	−68	119	172
fold plane	chiralities	τ_1[a]	τ_2	τ_3	τ_4	τ_5	τ_6	τ_7	τ_8	τ_9	τ_{10}	τ_{11}	
100	R, L	110.9	115.9	111.0	115.2	111.5	115.2	110.6	115.4	110.3			
100	R, R	111.4	120.5	113.5	120.0	102.9	116.3	100.7	126.8	109.5	112.3	106.4	
010	R, L	116.9	116.5	116.2	112.1	117.3	108.1	115.1	109.7	116.8	110.1	114.4	
010	R, R	104.0	114.3	109.8	115.2	111.3	115.6	108.5					
110	R, L	111.2	119.6	111.2	115.5	107.4	115.0	115.5	116.3	113.8	117.9	110.5	
110	R, R	111.1	116.3	109.2	115.2	110.8	115.4	110.8	111.5	111.7	116.0	110.3	

[a] The first variable bond angle τ_1 corresponds to a C−CH_2−C angle for the fold (010) R, L and to a C−$CH(CH_3)$−C angle for all the other folds.

Table 3. Minimum Energy Values of the Considered Folds (E_{fold}, in kJ·mol^{-1}) Calculated with Two Sets of Potential Functions

fold plane	chiralities	no. of bonds	E_{fold} (Flory)	E_{fold} (Scheraga)
100	R, L	10	62.4	49.6
100	R, R	12	94.4	85.5
010	R, L	12	64.0	50.9
010	R, R	8	47.1	36.1
110	R, L	12	137.5	99.7
110	R, R	12	66.1	54.4

of these two folds is not probable. The other folds, having lower and comparable energy values, are reasonable ways of realizing the chain folding. It should be noted that the values of E_{fold} ($=E_{conf} - E_{rif}$) obtained by our method of calculation can be considered an upper limit. In fact, we recall that E_{conf} values do not include attractive interactions between atoms of the starting and of the end chain in crystallographic positions. Moreover, the fold surface has been assumed to be rigid because we have kept even the atoms close to this surface fixed in the crystallographic positions. These atoms could be slightly displaced to relax possible interactions caused by short interatomic distances.

Views in a plane perpendicular to the chain axes and in the fold planes are shown for the best four folds in Figures 4−7. A close inspection of the two combined views evidences that no short intramolecular distances are present in any of these folds. Moreover, by looking at the steric encumbrance of the folds in the two views, it is possible to deduce that there is no strong interaction between the atoms of the fold and the atoms of adjacent chains in the crystalline regions, so that the packing efficiency is not perturbed. We have also verified, by our three-dimensional molecular models, that the atoms of the fold reported in Figures 4−7 are all far from the crystalline regions.

Conclusions

The results of our calculations indicate that adjacent re-entry folds can be realized at a low energy cost along the (010) plane and, with some restrictions, along (100) and (110) planes. In fact, the folds in the (100) and (110) planes are low in energy only if the chains have the opposite or the same chirality, respectively. Both conditions are realized in the *Ibca* space group. No condition on the chirality of the chains applies to the fold along the (010) plane, though the fold between chains having the same chirality has the lowest energy. We conclude

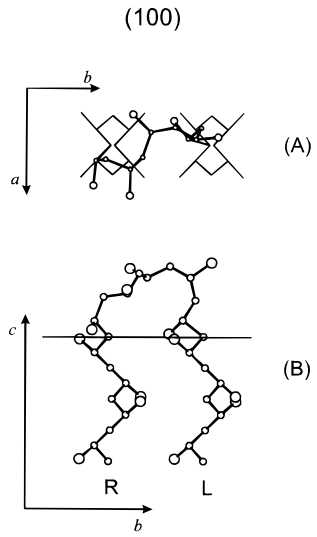

Figure 4. Projections along the chain axis (A) and in a direction perpendicular to the fold plane (B) for the minimum energy (100) R, L fold. The fold is indicated by balls and bold bonds in projection A. The horizontal line represents the trace of the fold surface in the projection B.

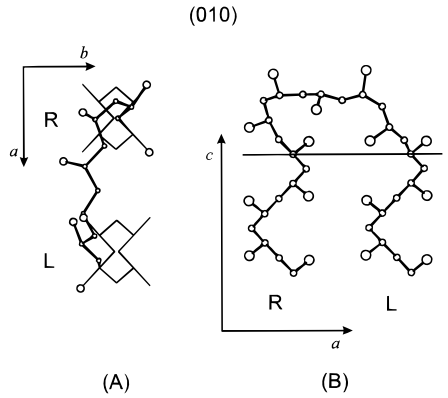

Figure 5. Projections along the chain axis (A) and in a direction perpendicular to the fold plane (B) for the minimum energy (010) R, L fold. The fold is indicated by balls and bold bonds in projection A. The horizontal line represents the trace of the fold surface in the projection B.

that only in the limit of an ordered structure, as in the *Ibca* space group, are folds along all three directions possible, while in the case of a statistical structure, proposed in ref 16, folds along *a* and *b* directions are preferred.

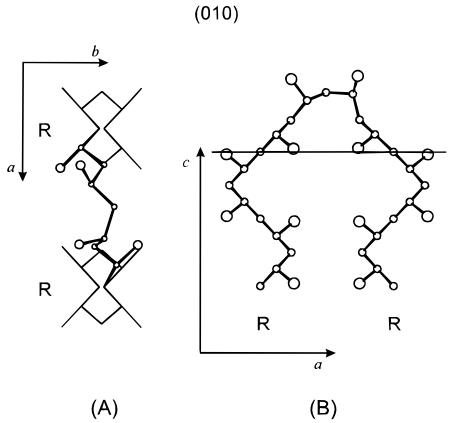

Figure 6. Projections along the chain axis (A) and in a direction perpendicular to the fold plane (B) for the minimum energy (010) R, R fold. The fold is indicated by balls and bold bonds in projection A. The horizontal line represents the trace of the fold surface in the projection B.

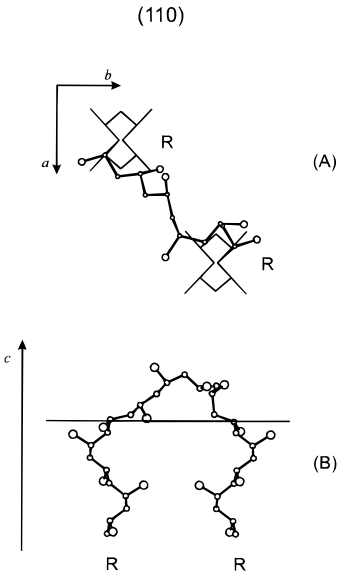

Figure 7. Projections along the chain axis (A) and in a direction perpendicular to the fold plane (B) for the minimum energy (110) R, R fold. The fold is indicated by balls and bold bonds in projection A. The horizontal line represents the trace of the fold surface in the projection B.

Some general features concerning the length of the folds result from our calculations. The number of bonds of the fold is not directly correlated to the distance between the chain axes, but it is dependent on the geometrical conditions dictated by the space group, i.e., chirality, relative orientation, and the difference in height of the chains linked by the fold. The folds having a lower number of bonds are lower in energy than longer folds.

Our results are in good agreement with experimental data. In fact, the values of E_{fold} obtained for the best four models are in good agreement with the work of fold q obtainable by the fold surface free energy σ_e in accordance with the formula $q = 2\sigma_e a_0 b_0$ where $a_0 b_0$ is the cross-sectional area (in our case 40.6 Å^2). Values of $\sigma_e \cong 100$ erg·cm^{-2}, corresponding to $q \cong 50$ kJ·mol^{-1}, have been obtained by measurements based on both linear crystal growth rates and overall isothermal crystallizations[42] on highly syndiotactic samples (% of pentads = 93.4). Lower values of q reported in the literature[33,43] were obtained on samples having a lower degree of syndiotacticity.

We have also examined the possibility of realizing models of folds which have a configurational defect corresponding to the presence of a *m* diad in a sequence ...*rrrr*.... The presence of more than one configurational defect is unlikely for tight folds (in our case, number of bonds ≤ 14) and for samples having a high degree of syndiotacticity ($n_{syn} \geq 20$). The configurational defect can be introduced in the model by removing or by adding a monomeric unit of the polymer, whatever is its configuration, in any part of the fold. A preliminary analysis has been confined to the best folds along the (100) planes. We have found that the best models are obtained by removing a monomeric unit both for the folds between chains having the opposite chirality and for the folds between chains having the same chirality. The optimized values of E_{fold} calculated with the non-bonded terms of Flory are 56.5 kJ·mol^{-1} for the (100) R, L fold composed of 8 bonds and 70.5 kJ·mol^{-1} for the (100) R, R fold composed of 10 bonds. The energy values are lower with respect to the corresponding values for the regular folds, and in particular, the energy of the R, R fold becomes almost comparable with the energy of the best regular folds. These results indicate that these configurational defects are easily tolerated along the *b* direction. A more complete study of the presence of configurational defects in the folds is in progress.

Acknowledgment. This work was supported by the Ministero dell'Università e della Ricerca Scientifica e Tecnologica, quota 40% (Italy).

Supporting Information Available: A table giving the values of torsion angles of the starting models (1 page). Ordering and access information is given on any current masthead page.

References and Notes

(1) Ewen, J. A.; Jones, R. L.; Razavi, A.; Ferrara, J. D. *J. Am. Chem. Soc.* **1988**, *110*, 6255.
(2) Immirzi, A.; De Candia, F.; Iannelli, P.; Vittoria, V.; Zambelli, A. *Makromol. Chem. Rapid Commun.* **1988**, *9*, 761.
(3) Lotz, B.; Lovinger, A. J.; Cais, R. E. *Macromolecules* **1988**, *21*, 2375.
(4) Greis, O.; Xu, Y.; Asano, T.; Petermann, J. *Polymer* **1989**, *30*, 590.
(5) Chatani, Y.; Maruyama, H.; Noguchi, K.; Asanuma, T.; Shiomura, T. *J. Polym. Sci., C: Polym. Lett.* **1990**, *28*, 393.
(6) Chatani, Y.; Maruyama, H.; Asanuma, T.; Shiomura, T. *J. Polym. Sci. B: Polym. Phys.* **1991**, *29*, 1649.
(7) De Rosa, C.; Venditto, V.; Guerra, G.; Pirozzi, B.; Corradini, P. *Macromolecules* **1991**, *24*, 5645.
(8) Pirozzi, B.; Napolitano, R. *Eur. Polym. J.* **1992**, *28*, 703.
(9) De Rosa, C.; Rapacciuolo, M.; Guerra, G.; Petraccone, V.; Corradini, P. *Polymer* **1992**, *33*, 1423.
(10) Chatani, Y.; Shimane, Y.; Inagaki, T.; Ijitsu, T.; Yukinari, T.; Shikuma, H. *Polymer* **1993**, *34*, 1620.
(11) Corradini, P.; De Rosa, C.; Guerra, G.; Napolitano, R.; Petraccone, V.; Pirozzi, B. *Eur. Polym. J.* **1994**, *30*, 1173.
(12) De Rosa, C.; Petraccone, V.; Dal Poggetto, F.; Guerra, G.; Pirozzi, B.; Di Lorenzo, M. L.; Corradini, P. *Macromolecules* **1995**, *28*, 5507.
(13) De Rosa, C.; Auriemma, F.; Corradini, P. *Macromolecules* **1996**, *29*, 7452.
(14) De Rosa, C.; Guerra, G.; Petraccone, V.; Pirozzi, B. *Macromolecules* **1997**, *30*, 4147.
(15) De Rosa, C.; Scaldarella, D. *Macromolecules* **1997**, *30*, 4153.
(16) Napolitano, R.; Pirozzi, B. *Polymer* **1997**, *38*, 4847.
(17) Sozzani, P.; Simonutti, R.; Galimberti, M. *Macromolecules* **1993**, *26*, 5782.
(18) Lovinger, A. J.; Lotz, B. *J. Polym. Sci. Polym. Phys.* **1997**, *35*, 2523.
(19) Hoffman, J. D.; Miller, R. L. *Polymer* **1997**, *38*, 3151.

(20) Sundararajan, P. R.; Kavassalis, T. A. *Macromolecules* **1997**, *30*, 5172.
(21) McMahon, P. E.; McCullough, R. L.; Schlegel, A. A. *J. Appl. Phys.* **1967**, *38*, 4123.
(22) Petraccone, V.; Allegra, G.; Corradini, P. *J. Polym. Sci. C* **1972**, *38*, 419.
(23) Conte, G.; D'Ilario, L.; Pavel, N. V.; Giglio, E. *J. Polym. Sci. Polym. Phys.* **1979**, *17*, 753.
(24) Giglio, E.; Morosetti, S.; Palleschi, A.; Pavel, N. V. *J. Polym. Sci. Polym. Phys.* **1983**, *21*, 321.
(25) Petraccone, V.; Pirozzi, B.; Meille, S. V. *Polymer* **1986**, *27*, 1665.
(26) Petraccone, V.; Pirozzi, B.; Meille, S. V. *Eur. Polym. J.* **1989**, *25*, 43.
(27) Schmieg, C.; Grossmann, H. P.; Hägele, P. C. *Polymer* **1990**, *31*, 631.
(28) Ihn, K. J.; Tsuji, M.; Isoda, S.; Kawaguchi, A.; Katayama, K. *Macromolecules* **1990**, *23*, 1788.
(29) Chum, S. P.; Knight, W.; Ruiz, J. M.; Phillips, P. J. *Macromolecules* **1994**, *27*, 656.
(30) Lovinger, A. J.; Davis, D. D.; Lotz, B. *Macromolecules* **1991**, *24*, 552.
(31) Lovinger, A. J.; Lotz, B.; Davis, D. D.; Padden, F. J., Jr. *Macromolecules* **1993**, *26*, 3494.
(32) Lovinger, A. J.; Lotz, B.; Davis, D. D.; Schumacher, M. *Macromolecules* **1994**, *27*, 6603.
(33) Rodriguez-Arnold, J.; Bu, Z.; Cheng, S. Z. D.; Hsieh, E. T.; Johnson, T. W.; Geerts, R. G.; Palackal, S. J.; Hawley, J. R.; Welch, M. B. *Polymer* **1994**, *35*, 5194.
(34) Tsukruk, V. V.; Reneker, D. H. *Macromolecules* **1995**, *28*, 1370.
(35) Thomann, R.; Wang, C.; Kressler, J.; Jüngling, S.; Mülhaupt, R. *Polymer* **1995**, *36*, 3795.
(36) Loos, J.; Buhk, M.; Petermann, J.; Zoumis, K.; Kaminsky, W. *Polymer* **1996**, *37*, 387.
(37) Bu, Z.; Yoon, Y.; Ho, R.; Zhou, W.; Jangchud, I.; Eby, R. K.; Cheng, S. Z. D.; Hsieh, E. T.; Johnson, T. W.; Geerts, R. G.; Palackal, S. J.; Hawley, J. R.; Welch, M. B. *Macromolecules* **1996**, *29*, 6575.
(38) Corradini, P. in *Stereochemistry of Macromolecules*; Ketley, A., Ed.; Marcel Dekker: New York, 1968; Part III, p 1.
(39) Really, in this case the length of the vector translation becomes the *b* axis of a halved unit cell.
(40) Scott, R. A.; Scheraga, H. A. *J. Chem. Phys.* **1966**, *45*, 2091.
(41) Pletnev, V. Z.; Popov, E. M.; Kadymova, F. A. *Theor. Chem. Acta* **1974**, *35*, 93.
(42) Silvestre, C.; Di Pace, E. Private communication.
(43) Miller, R. L.; Seeley, E. G. *J. Polym. Sci., Polym. Phys.* **1982**, *20*, 2297.

MA971872X